Inertia emulation with the concept of virtual supercapacitor based on SOC for distributed storage systems in islanded DC microgrid

Piri Yengijeh, Navid; Moradi CheshmehBeigi, Hassan; Hajizadeh, Amin

Published in:
IET Renewable Power Generation

DOI (link to publication from Publisher):
10.1049/rpg2.12537

Publication date:
2022

Document Version
Publisher's PDF, also known as Version of record

Received: 18 February 2022 | Revised: 25 May 2022 | Accepted: 17 June 2022

DOI: 10.1049/rpg2.12537

IET Renewable Power Generation

The Institution of Engineering and Technology WILEY

ORIGINAL RESEARCH

Inertia emulation with the concept of virtual supercapacitor based on SOC for distributed storage systems in islanded DC microgrid

Navid Piri Yengijeh[1] | **Hassan Moradi CheshmehBeigi**[1] | **Amin Hajizadeh**[2]

[1]Electrical Engineering Department, Razi University, Kermanshah, Iran

[2]Department of Energy Technology, Aalborg University, Esbjerg, Denmark

Correspondence
Tagh-e-Bostan, University St., Kermanshah 6714414971, Iran.
Email: ha.moradi@razi.ac.ir

Abstract

One of the main crises that the world will face is the over pollution of the environment due to the use of fossil fuels. This problem will be solved by replacing renewable energy sources (RESs). DC microgrids (DCMGs) provide the ability to exploit all the potential of RESs. But, high penetration of these sources reduces the inertia and damping of the DCMGs. Therefore, it makes DCMG vulnerable to fluctuations and disturbances. This challenge can be addressed by using distributed energy storage systems (DESS) in DCMGs and inertial simulations. To improve the inertia as well as to balance the charge/discharge of the DESS, the concept of a virtual supercapacitor based on the state of charge (SOC) is introduced. Under the proposed control strategy, DCMG inertia is provided and the SOC balance is maintained in charge and discharge mode. Due to the bidirectional power transmission capability, symmetrical structure and considering the protection purposes of dual half-bridge converter (DHB) can be selected. A small signal has also been investigated to analyse the role of virtual inertia in stability. The simulation results in MATLAB/Simulink show the correct performance dynamics and high impact of the proposed scheme compared to conventional schemes.

1 | INTRODUCTION

The exploitation of renewable energy sources (RESs) is a confident way to overcome the energy crisis and reduce environmental problems. DC microgrids (DCMGs) provide the ability to exploit all the potential of RESs. Therefore, they have been studied as a worthy model and a suitable alternative. The advantages of MGs include increasing power quality, facilitating distribution, improving reliability, and reducing environmental pollutants [1–3]. AC microgrids (ACMGs) have problems, such as reactive power control. It also consists of several complex AC/DC and DC/AC converters, which makes it less popular [4–6]. On the other hand, RESs as the main part of power generators and often as DC microgrid (DCMG) consumers have the ability to generate and consume power as DC, and this, among other benefits, increases the utilization of DCMG. Therefore, the future cannot be imagined without DCMGs [7, 8].

Rotational inertia decreases with the presence of RESs in DCMGs. Lack of inertia makes DCMG prone to voltage and power fluctuations. So, controlling them will be a serious challenge. To maintain proper system operation, the voltage must be in the safe range. Therefore, in the absence of real inertia, the concept of creating inertia will be expressed virtually. The presence of distributed energy storage systems (DESSs) along with electronic power converters (PECs) and a suitable control mechanism has significant potential in providing services to solve the problems mentioned. Inertial emulation methods have been less studied in DCMGs than in ACMGs. However, research on the inertial emulation of DCMGs has become an interesting topic and several fields of research have been identified.

In [9], by placing a decentralized inertia loop and controlling the active power based on photovoltaics (PV), virtual inertia can be provided to DCMG. Inertia simulation has been studied by DC link capacitors and wind turbines [10]. Virtual inertia supply methods to improve inertia and damping with negative feedback as well as the use of energy stored in ESSs for DCMG have been investigated, respectively [11, 12]. Through the energy storage system (ESS), energy is stored in the generator rotor Permanent magnet synchronize generator (PMSG) with a high-pass filter

can improve voltage fluctuations. However, this method is sensitive to voltage differential and incorporates it into the control strategy [13]. In [14], a virtual inertia strategy is expressed in DCMG. Due to the use of DCMG by simulating DC machines, inertia can be provided to DCMG. Therefore, in [15], by simulating the simplest type of DC machine, inertia is provided to DCMG. By analysing the specifications of the compound dc machine in [16], the governing relationships of this machine are simulated. In addition to the many advantages of this proposed design, the use of the buck-boost converter with normal efficiency, lack of electrical insulation and nonconsideration of the protective purposes of batteries can be named as factors that need further research. It is also necessary to consider the charge and discharge status of the batteries as an important part of the inertia imitation unit to increase the life and productivity of the batteries. An inertia emulation strategy is proposed using the modelling of a separately excited DC machine considering the SOC of the batteries [17]. In this design, the buck-boost converter is used as an interface converter with DCMG, as well as considering the charging and discharging status of batteries. In [18, 19], a virtual inertia strategy is proposed to provide inertia. However, batteries, as an important part of inertia emulation, need more protection than before. Therefore, it is necessary to protect the batteries by isolating them in the event of an error.

Real supercapacitors with sufficient inertia can provide a DCMG interface alone and even without the need for a converter. However, high cost, protection problems and high discharge itself are all limiting factors of the supercapacitor that make them difficult to use [20]. An ESS that is connected to the DC bus via PEC can be used as an inertial emulation unit. The low self-discharge rates, low cost and the ability to deliver power for a long time are the advantages of batteries [21, 22]. Problems with batteries include overcharging and discharging, and a lack of attention to the state of charge (SOC) balance in DESSs. Therefore, to increase efficiency, increase battery life, save costs and provide important loads, it is desirable that the SOC of batteries should always be considered as power management [23, 24]. In [25] the SOC balance is examined with the dynamic average consensus (DAC) approach. An improved droop control strategy is expressed in [26] for SOC better balance. In [27], the ESS management method is expressed through power management and secondary control for charge and discharge balance. In explaining power management, it can be stated that the SOC control method based on charge and discharge mode for DESSs to achieve proper power distribution, droop control as a decentralized approach, and based on power distribution method has been used for DESSs. In [28] the local droop coefficient with inverse SOC^n is proposed for power distribution. But this method considers the power balance only in the mode of discharge ESSs. In [29], the droop coefficient is controlled proportionally or inversely SOC^n to create power balance in charge and discharge mode. However, conventional droop controls lack damping and inertia simulation properties. By studying the mentioned schemes, it can be said that inertia supply can be classified into three main methods. The first is to simulate rotating machines and use their inertia term along with ESS, then the presence of the real supercapacitors, as well as the use of inertia in rotating objects such as wind turbines can be partially provided. But in order to consider protection purposes as well as high efficiency along with the lack of control complexity, the need for an isolated bidirectional converter and an efficient control scheme is felt more than ever. These factors can also be mentioned as the lack of previous schemes.

Therefore, controllers must be defined that provide the required inertia to the DCMG while maintaining power balance. To overcome the mentioned challenges to improve DCMG inertia and power balance in mode charge/discharge and ESSs, by integrating [29], a virtual supercapacitor control strategy based on SOC is presented for DESSs in DCMGs. Due to the simple control, a low number of components and low cost, bidirectional power transmission capability and symmetrical structure of dual half-bridge (DHB) converter have been used [30, 31]. Virtual supercapacitor based on SOC is an intelligent, efficient and reliable strategy. The proposed scheme balances power and SOC at the same time. Therefore, the inertial response of the system is improved and the life of the batteries is increased. The purpose of this article is as follows:

- Improve DC bus voltage stability by increasing inertia in DCMG.
- Simulation of inertia using virtual supercapacitor strategy and DESSs in DCMG.
- Availability of important terms for inertia emulation without the complexities of rotating machines.

The remaining of this article is as follows. Section 2 describes the structure of DCMG; Section 3 describes the concept of virtual inertia and supercapacitor modelling. Section 4 describes the virtual supercapacitor. Section 5 examines the small signal. Finally, in Sections 6 and 7, the simulation results and conclusions of the paper are presented.

2 | DESCRIPTION AND MODELLING OF DCMG STRUCTURE

The schematic of DCMG simulated in MATLAB/SIMULINK is shown in Figure 1. DCMG includes a wind turbine (WT) based on a PMSG capable of supplying 5.5 kW. A photovoltaic (PV) also provides DCMG power with a rated power of 7 kW. Both of these units provide DCMG with the desired power through boost converters at the appropriate voltage. Due to the variable power generation of the mentioned units and also to further confirm the simulation results, the fuel cell (FC) unit has been used to supply power in DCMG. This unit has the ability to supply a nominal power of 6 kW. All of these components are connected by PECs to a DC bus with a voltage of 400 V. Each inertia emulation unit consists of two 96 V series batteries and a DHB. These units adjust the input and output according to the voltage of the DC bus and control the charge and discharge of the batteries. These units can support the system with a nominal power exchange of 7.5 kW. In general, the load can have a

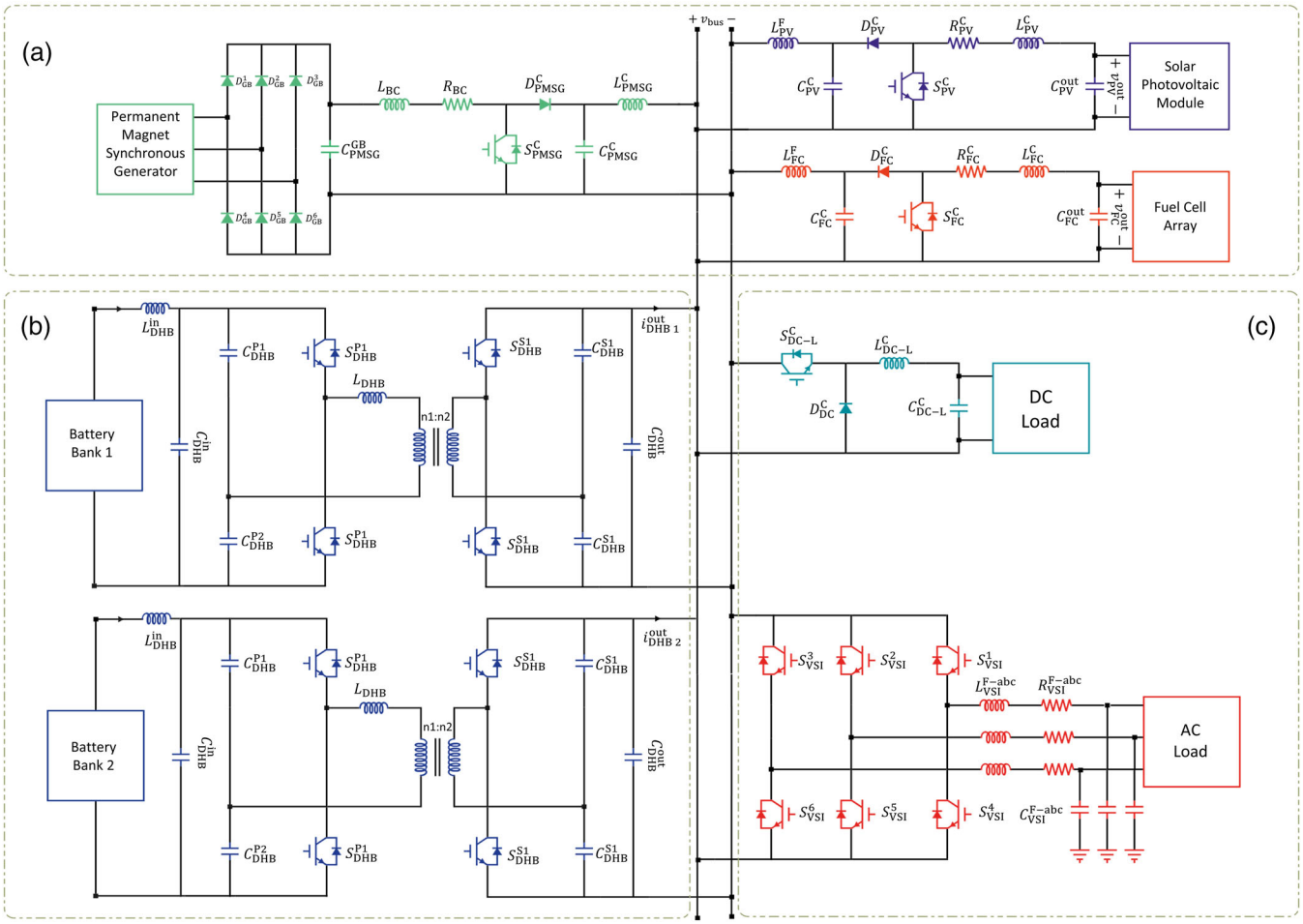

FIGURE 1 Accurate structure and configuration DCMG (a) DGs: WT, PV and FC units, (b) Support: virtual supercapacitor, (c) loads: AC and DC load units

maximum demand of up to 15 kW. In DCMG, a Buck converter with a current controller is used to transfer power to DC load at the appropriate voltage. The AC load set will also be powered via a voltage source inverter (VSI) connected to a DC bus. Other DCMG parameters are collected in Table 1.

3 | THE CONCEPT OF VIRTUAL INERTIA AND SUPERCAPACITOR MODELING

The rotor of real synchronous generators as a rotating and heavy object provides natural and inherent inertia to the system. The governing equation of the rotor of these rotary machines is as follows:

$$W_r = \frac{1}{2} J(\omega_r^m)^2 \tag{1}$$

In this equation, J represents the term inertia. W_r and ω_r^m are the kinetic energy stored in the machine rotor and the angular velocities of the rotor, respectively. Now, if the energy equation governing the capacitor is examined, the common terms with Equation (1) are determined.

$$W_c = \frac{1}{2} C(V)^2 \tag{2}$$

In this equation, W_c is the electrical energy stored in the capacitor. C represents the capacitance of capacity and V represents the capacitor voltage. With accuracy in Equations (1) and (2), the energy of the capacitor and the energy of the rotor can be assumed to be equal. The equivalence of these two equations can be written:

$$\frac{1}{2} J(\omega_r^m)^2 \equiv \frac{1}{2} C(V)^2 \tag{3}$$

with accuracy in this equation, it can be seen that a capacitor similar to a rotary machine rotor can operate. This property is obtained due to the resistance of the capacitor against voltage change. Therefore, the capacitor can convert this quantity to an accessible quantity for the system by preserving the important parts for emulation inertia. This is especially important because the capacitor governing equation can be easily used in DCMGs. Therefore, it is necessary to implement a virtual inertia control

TABLE 1 Parameters of DCMG units

Unit	Parameter	Symbol	Magnitude/type
WT	Nominal speed	v^{N}	12 m/s
PMSG	Nominal power	P^{N}_{PMSG}	5.5 kW
	Nominal torque	T^{N}_{PMSG}	24 N.m
	Nominal angular velocity	ω^{N}_{PMSG}	2,300 rpm
	Number of poles	P_{PMSG}	4
PV	Number of cells per module	n_{cell}	72
	Power of each module	P^{N}_{M}	150 w
	Nominal power	P^{N}_{PV}	7 kW
FC	Type	–	Solid oxide
	Nominal power of each stack	P^{N}_{FC}	3 kW
	Nominal voltage of each stack	V^{N}_{FC}	100 V
	Number of stacks in each array	n_{FC}	2
	Nominal power of the array	P^{N}_{FC}	6 kW
Battery	Type	–	Lead-acid
	Capacity	C^{N}_{Bat}	50 Ah
	Nominal voltage	V^{N}_{Bat}	96 V
	Number of batteries per pack	n_{Bat}	2 (Series)

strategy by examining the governing equation of the capacitor to use it to simulate inertia:

$$I_C = C_v \frac{dv}{dt} + G_v(V) \tag{4}$$

In this equation, C_v is the capacity of the virtual capacitor and G_v is the capacity of the virtual conductor. V and I_C are the capacitor voltage and the virtual capacitor current, respectively.

To inertia emulation, it must be possible to place the properties of Equation (4) in the PEC control system. In other words, the power exchange between the battery and the DCMG must have the power exchange characteristics of a real supercapacitor with high inertia. This means that from a DCMG perspective, there is not much difference between a battery controlled by an inertial emulation scheme and a real supercapacitor. The inherent parameters of a real supercapacitor such as inertia and damping are converted into control parameters that can be easily modified according to DCMG. In addition, the removal of undesirable properties of ESSs such as low power density and real supercapacitor will ensure the stability of DCMGs.

4 | VIRTUAL SUPERCAPACITORS BASED ON SOC

With the increasing growth of distributed generations (DGs), the control of DCMGs is a concern for researchers, given that these sources do not have a heavy rotational mass. One way to control and increase the stability of DCMGs in this case is to add inertia virtually. Virtual inertia can be created using appropriate PECs, ESSs and control mechanisms. As a result, the concept of virtual inertia will be crucial for the participation of DGs in Modern and novel DCMG without compromising DCMG stability. The virtual supercapacitor based on SOC unit provides suitable inertia and damping specifications for DCMG. The following sections describe the structure of the inertia emulation unit and the operation of this unit, respectively.

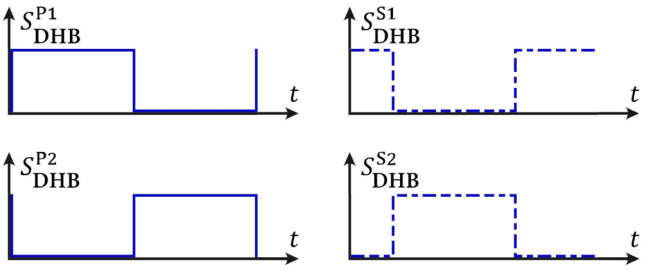

FIGURE 2 DHB converter SPS switching technique

4.1 | Structure

The virtual supercapacitor based on SOC consists of three basic components: the ESS, the converter and a control mechanism in the control block of the virtual supercapacitor unit, is placed a dynamic function similar to the exact equation of the capacitor. In this unit, a DHB converter is considered a DC–DC converter to enable power transfer. This converter is connected to Two 96 V series batteries on the primary side. On the other side of this converter is the DC bus. These batteries are of the lead-acid type with a capacity of 50 Ah. All values are listed in Table 2. A DHB converter consists mainly of two half-bridges, a high-frequency transformer and input and output filters. The DHB converter can transfer power in both directions by using two independent DC/AC half-bridge that connect together with high-frequency transformer. Features such as low weight, cost reduction, voltage level adjustment and prevention of core saturation, make this type of transformer a good option for making DHB converters. This converter consists of four power switches. Due to high efficiency, IGBT power switches have been used. The output of the first bridge is connected to the transformer via auxiliary inductance. Auxiliary inductance is installed in the circuit to store instantaneous energy and help with the inductances of the transformer windings. Capacitive filters are used at the beginning and end of this converter. The phase-shifted (PS) method is one of the simple yet practical methods that can achieve zero voltage switching (ZVS) in specific ranges. This method is mainly used. The conduction pulses for the PS method are shown in Figure 2. It should be noted that the two conduction pulses of the second half-bridge have a general difference with the two conduction pulses of the first bridge. This phase difference is called the external phase difference, which is the main factor determining the amount and direction of

TABLE 2 Characteristics of virtual supercapacitor parameters

Section				Symbol	Magnitude
Physical structure		Type		–	DHB
		Switch type		—	IGBT/Diode
		Auxiliary inductance		L_{DAB}^{aux}	4.3 μH
		Filter capacitor		C_{DHB}^{in}	1.5 mF
				C_{DHB}^{out}	1.5 mF
				$C_{DHB}^{p1,2}$	100 μF
				$C_{DHB}^{s1,2}$	100 μF
	Transformer	Nominal power		—	7.5 KVA
		Turns ratio		n	96/400
		Switching frequency		f_s	5 kHz
		Primary	Winding resistance	R_{DHB}^{P}	Ignored
			Winding inductance	L_{DHB}^{P}	0.5 μH
		Secondary	Winding resistance	R_{DHB}^{S}	Ignored
			Winding inductance	L_{DHB}^{S}	2 μH
		Core resistance		R_{DAB}^{core}	12,500 Ω
		Leakage inductance		L_{DAB}^{leak}	80 mH
Controller		Proportional-integral Voltage controller		$k_{VSC}^{P_V}$	50.923
				$k_{VSC}^{I_V}$	350.1614
	Virtual capacitor	Virtual capacitor		C_v	0.002
		Virtual conductor		G_v	0.5
		Low pass filter		—	10 kHz
		Proportional-integral current controller		$k_{VSC}^{P_i}$	0.0866
				$k_{VSC}^{I_i}$	28.426

transmission power in this type of converter. The equation of active transfer power in DHB converter (P_DHB) will be as follows [32]:

$$P_{DHB} = \frac{nV_1V_2}{8\pi^2 f_s L}\varphi(\pi - |\varphi|) \quad (5)$$

Indicates the number of transformers round, f_s is the switching frequency V_1 and V_2 RMS values of input and output voltages, φ external phase difference. L Total auxiliary inductance and leakage inductance at the primary side. Therefore, by selecting the appropriate value φ, the amount and direction of the active transmission power can be easily determined.

5 | OPERATION

Providing inertia and paying attention to the SOC of batteries is the aim of the SOC-based virtual supercapacitor scheme. The control unit consists of parts, a double quadrant droop controller, voltage controller, inertia emulation unit and current control unit. In the double quadrant droop control unit, in charge and discharge mode, the power is adjusted according to the charge amount of each ESS by changing the voltage reference value. In the charging process, the droop coefficient is proportional to SOC^n, while in the discharge process, the dropping coefficient is set inversely to the order SOC^n. The amount of power received or delivered from ESSs depends on their SOC. This amount of power can be specified according to the drop coefficient. In the charging process, the power and drop coefficients are inversely proportional. Therefore, it is clear that each ESS unit with a higher SOC receives less power than the other ESS unit. In the discharge process, due to the fact that the drop coefficient is directly proportional to the power of the ESSs, this makes the ESS with SOC more DCMG power. Therefore, power balance will be achieved in the use of ESSs. The block diagram of the virtual supercapacitor based on SOC control unit is shown in Figure 3. The voltage control unit is the first control unit. This unit generates a virtual supercapacitor voltage by comparing the reference and measured voltages and passing through the proportional-integral controller (PI). Adjusting the frequency of the first-order low-pass filter (LPF) for the first time prevents the addition of high-oscillation disturbances to the control system. The voltage generated in the previous section determines the current of the supercapacitor by passing through the equation governing the real capacitor. This creates a battery reference current. The current controller sends the output for switching after passing through the pulse width modulation unit (PWM) by comparing the reference current and the measured current. Proper adjustment of the PI

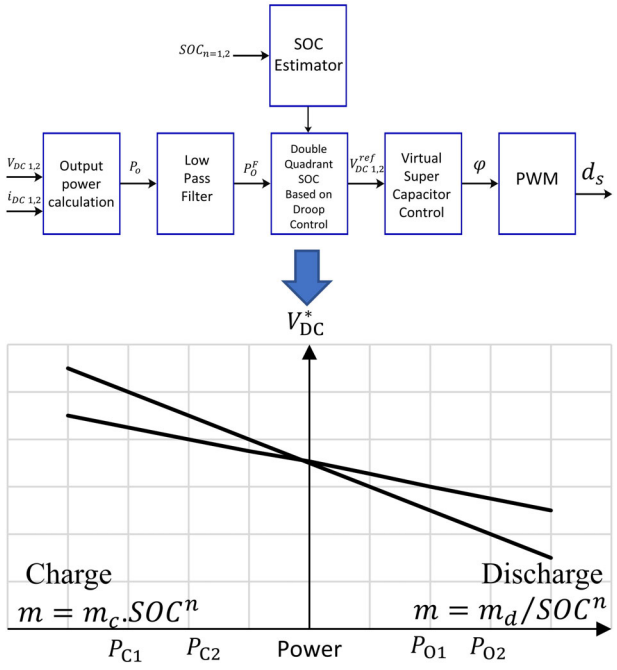

FIGURE 3 Double quadrant operation of ESSs, with quadrant I shows the discharging operation mode and quadrant II shows the charging operation mode.

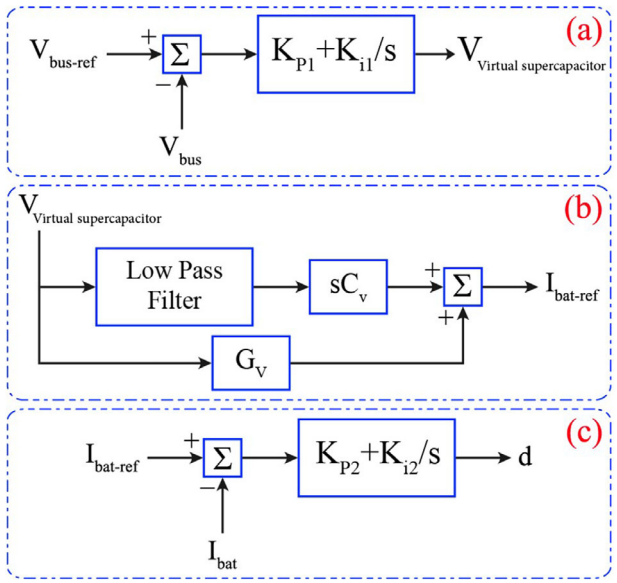

FIGURE 4 Block diagrams control: (a) voltage controller, (b) virtual capacitor controller, (c) current controller.

controller prevents excessive delays or large fluctuations. The block diagram of this unit is shown in Figure 4.

The virtual supercapacitor based on SOC can operate in a variety of modes, suppressing fluctuations by exchanging power, and giving DCMG stability. Therefore, this unit reacts to the DC bus to issue the necessary command to exchange power. By knowing the power generation units and consumers, the power equation can be expressed in DCMG. It is clear that the operation of the virtual supercapacitor unit SOC based can vary according to the power equation. The power equation is expressed as follows:

$$P_{\mathrm{VSC}}^{\mathrm{out}} = P^{\mathrm{gen}} - P^{\mathrm{load}} \tag{6}$$

$$P^{\mathrm{load}} = P_{\mathrm{AC-L}} + P_{\mathrm{DC-L}} \tag{7}$$

$$P^{\mathrm{gen}} = P_{\mathrm{PMSG}}^{\mathrm{gen}} + P_{\mathrm{PV}}^{\mathrm{gen}} + P_{\mathrm{FC}}^{\mathrm{gen}} \tag{8}$$

which $P_{\mathrm{PMSG}}^{\mathrm{gen}}$, $P_{\mathrm{PV-A}}^{\mathrm{gen}}$ and $P_{\mathrm{FC}}^{\mathrm{gen}}$ are the output power of WT, PV and FC, respectively, as well as $P_{\mathrm{AC-L}}$ and $P_{\mathrm{DC-L}}$ is the power consumption of the AC and DC load. To adjust the voltage at the reference value and the power balance, production and consumption must be balanced. However, the difference between production capacity and demand is inevitable. Support units are able to meet this challenge. $P^{\mathrm{gen}} > P^{\mathrm{load}}$ when the output power is more than the required power. In this case, the DC bus experiences an undesirable voltage deviation. The backup units are in charging mode and save extra power at any time. When the load power is not supplied with the output power of the resources, $P^{\mathrm{gen}} < P^{\mathrm{load}}$ will be. In this case, the DC bus has a voltage drop. To solve this problem, the backup units compensate for the power shortage by injecting power through discharge and preventing voltage deviation. When the power balance between supply and demand, $P_{\mathrm{VSC}}^{\mathrm{out}} = 0$.

That is, the virtual capacitor super unit will not exchange power. In this case, the DC bus voltage is set exactly to its reference value. Therefore, the backup units operate during operation to maintain the stability of the system. In addition, by integrating DESSs in DCMG, the limitations of RESs power generation are compensated.

6 | STABILITY ANALYSIS AND DESIGN OF VIRTUAL SUPERCAPACITOR CONTROLLER

Small signal analysis is an important step in reviewing and feasibility of the proposed scheme. Therefore, by analysing all the parts of the specified unit, the transfer function of different parts can be calculated. Then, using the superposition theorem and Mason's rule, the total transfer function of the system can be calculated. After that, the stability of the system can be checked with various methods and tools. The accuracy of the small-signal model of these groups of converters has been investigated in [33, 34].

$$G_{v_{\mathrm{bus}}v_{\mathrm{bat}}}\%\,(s) = \frac{\left(g\left(\left(\frac{1}{D}\right) + \frac{gsL_{\mathrm{DC}}}{D^2}\left(\frac{SC_{\mathrm{p}}}{2D\left(1+s^2\frac{C_{\mathrm{p}}}{2}L_{\mathrm{DC}}\left(\frac{1}{D}\right)^2\right)}\right)\right)\right)}{\left(s\frac{C_{\mathrm{t}}}{2} + \frac{gsL_{\mathrm{DC}}}{D^2}\left(\frac{g}{2D\left(1+s^2\frac{C_{\mathrm{p}}}{2}L_{\mathrm{DC}}\left(\frac{1}{D}\right)^2\right)}\right)\right)} \tag{9}$$

$$G_{\dot{v}_{\text{bus}}\dot{i}_{\text{bus}}}(s) = \frac{1}{\left(s\frac{C_t}{2} + \frac{gsL_{DC}}{D^2}\left(\frac{g}{2D\left(1+s^2\frac{C_p}{2}L_{DC}\left(\frac{1}{D}\right)^2\right)}\right)\right)} \tag{10}$$

$$G_{\dot{v}_{\text{bus}}\varphi}(s) = \frac{\left(-n - \frac{gsL_{DC}}{D^2}\left(\frac{m}{2D\left(1+s^2\frac{C_p}{2}L_{DC}\left(\frac{1}{D}\right)^2\right)}\right)\right)}{\left(s\frac{C_t}{2} + \frac{gsL_{DC}}{D^2}\left(\frac{g}{2D\left(1+s^2\frac{C_p}{2}L_{DC}\left(\frac{1}{D}\right)^2\right)}\right)\right)} \tag{11}$$

$$G_{\dot{i}_{\text{bat}}\dot{i}_{\text{bus}}}(s) = \frac{-2g}{sC_t\left(1 + s^2\frac{C_p}{2}L_{DC}\left(\frac{1}{D}\right)^2\right) + \frac{2g}{D^2}L_{DC}sg} \tag{12}$$

$$G_{\dot{v}_{\text{bat}}\dot{i}_{\text{bat}}}(s) = \frac{sC_t\left(sC_p\left(\frac{1}{D}\right) + 2g^2\left(\frac{1}{D}\right)\right)}{sC_t\left(1 + s^2\frac{C_p}{2}L_{DC}\left(\frac{1}{D}\right)^2\right) + \frac{2g}{D^2}L_{DC}sg} \tag{13}$$

$$G_{\dot{i}_{\text{bat}}\varphi}(s) = \frac{sC_t n + 2n}{C_t\frac{C_p}{2}L_{DC}\left(\frac{1}{D}\right)^2 s^3 + \frac{2g}{D^2}C_t L_{DC}gS^2 + sC_t} \tag{14}$$

The transfer functions of the controller are defined as follows:

$$G_{c1}(s) = \frac{V_{\text{vsc}}}{\Delta V} = \left(k_{P_V} + \frac{k_{I_V}}{s}\right) \tag{15}$$

$$G_{c2}(s) = \frac{I_{\text{bat}}^{\text{ref}}}{V_{\text{vsc}}} = \left(G_v + \frac{1}{1+TS}sC_v\right) \tag{16}$$

$$G_{c3}(s) = \frac{,}{\Delta I_{\text{bat}}} = \left(k_{P_I} + \frac{k_{I_I}}{s}\right) \tag{17}$$

The total transfer function of the system is as follows:

$$G_{uo}(s) = \frac{G_{c1}(s)\,G_{c2}(s)\,G_{c3}(s)\,G_m(s)\,G_{\hat{\varphi}}^{\hat{v}_{\text{bus}}}(s)}{1 + G_{c3}(s)\,G_{\hat{\varphi}}^{\hat{i}_{\text{bat}}}(s) + G_{c2}(s)\,G_{c3}(s)\,G_m(s)\,G_{\hat{\varphi}}^{\hat{v}_{\text{bus}}}(s)} \tag{18}$$

6.1 | Adjust virtual supercapacitor controller

To examine the small signal of the controller added to the model, by keeping all the controller parameters constant and only changing the value of one parameter, the effect of changes in that parameter on system stability can be seen. In this regard, the effect of control parameters C_V and G_V was examined separately. To start, using MATLAB software, the step response diagram for C_V can be drawn. The results in MATLAB software are shown in Figure 5. As can be seen, by increasing the value of C_V, rise time, settling time and the steady-state response of the desired transfer functions are simultaneously improved, and consequently, the stability of the system will be increased. However, increasing the value of C_V too much can cause a lot of inertia in the system, which in turn causes changes in the power balance of the system. The DC bus voltage value is too slow to reach its reference value. Also, too fast the system will cause problems. Therefore, a value of 0.002 is considered for C_V, which provides good stability for the system. The step

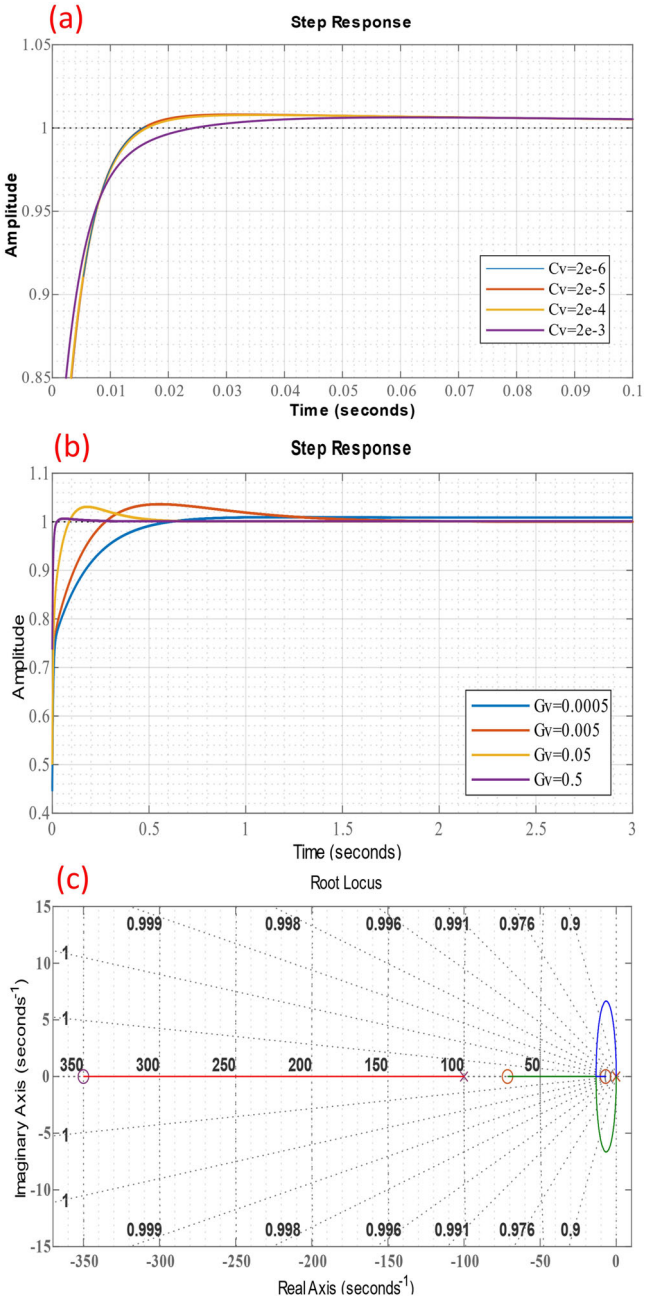

FIGURE 5 Small signal analysis: (a) step response controller transfer function, (b) step response controller transfer function, (c) root LOCUS plot controller transfer function.

response diagram is also used to determine the value of the G_V parameter. As shown in Figure 5a, by increasing the value of G_V, the rise Time, the settling time and the final value of the step response will be at its best, and with a very low rise time, it will reach its final value. In contrast, in other values of G_V, the response of the conversion function step will be very long, and the system will also fluctuate. Therefore, a value of 0.5 is considered for G_V, which provides good stability for the system. From Figure 5, it can be concluded that virtual inertia is stable in a certain range and increasing damping causes damping of DCMG fluctuations and increases DCMG stability. As the gain increases, the closed loop poles move to the left of the imaginary axis. None of the branches of the Root Locus tend to the right, and the Root Locus branches remain on the left. Therefore, by examining the control small signal as well as examining the step response diagrams and the Root Locus, it can be stated that the system is stable.

7 | SIMULATION RESULTS

In the DCMG, in the load change scenario with balanced SOC, the ability of the proposed scheme to voltage control has been investigated. Then, the proposed scheme is tested with an unbalanced SOC during the load change scenario. Power generation sources (WT, PV and FC) provide DCMG with constant power until the end of the simulation. The WT supplies 4.5 kW of power, which is approximately equivalent to 33% of DCMG power. The PV also provides 6 kW for most of the charge, which is about 45%. The FC responds to another part of the load demand by generating 3 kW. The total AC and DC loads reach a maximum of 15 kW. The connection of generations, loads and backup units is shown in Figure 6.

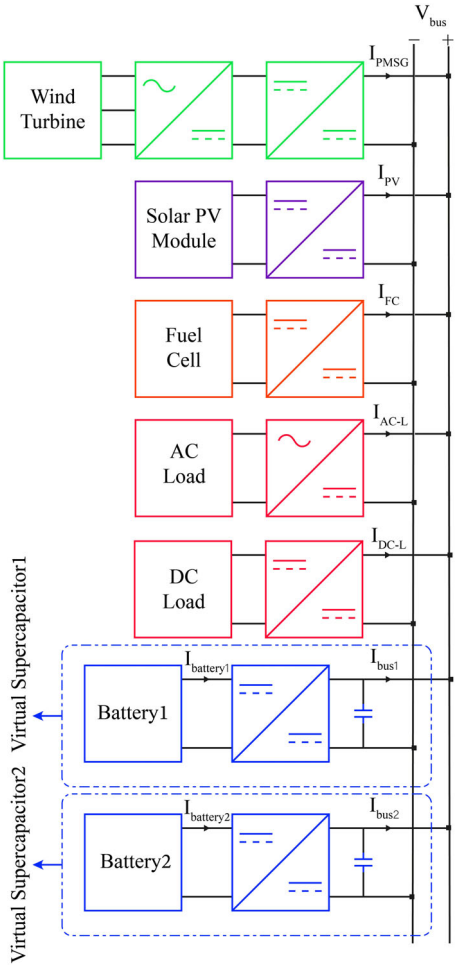

FIGURE 6 Power system diagram DCMG

7.1 | Performance of virtual supercapacitor based on SOC unit with balanced SOC

Initially, DCMG is started with a load of 12 kW. In this case, the power generated from the sources shows the number 13.5 kW. As shown in Figure 7a, the extra power is stored by the virtual supercapacitor unit. As shown in Figure 7b,c, the battery power is negative and this indicates that these units are in charging mode. After 0.4 s, 1.5 kW is added to the DCMG load. In this case, the bus voltage drops and, as shown in Figure 7a, the virtual supercapacitor units return the voltage by exchanging power and no longer have power exchange with DCMG. In the next step, 1.5 kW is added again. In this case, the loads reach their maximum value, and this causes the bus voltage to drop again. This time, the virtual supercapacitor units return the bus voltage to its reference value by exchanging power and more precisely by discharging. As shown in Figures 8b,c, the battery power of these units is positive. At 1.2 and 1.6, the added loads are disconnected from the DCMG, and as the loads are cut off, the voltage increases, which is suppressed by the virtual supercapacitor units. In moments of load change, the compound s scheme is also acceptable with a larger drop than the virtual supercapacitor scheme, but in order to improve the inertia emulation and other mentioned factors, using the proposed scheme leads to better results. As shown in Figures 7 and 8, the proposed scheme meets this challenge with the correct exchange of power at load change moments. The proposed scheme, in addition to reducing voltage changes at power change moments, does not have the complexity of the scheme [16]. This factor simplifies the adjustment of control parameters. The presence of an isolated converter also protects the batteries as an important and costly part of DCMG in the event of a fault. In addition, considering the SOC of batteries improves the performance and efficiency of batteries. Table 3 express details of the

TABLE 3 Comparison of simulation results

	Proposed scheme	Compound scheme [16]	Conventional scheme
0.4	0.41484	0.90443	2.77353
0.8	0.40895	0.94548	3.46446
1.2	0.33647	0.93239	2.90218
1.6	0.36499	0.91619	2.81593

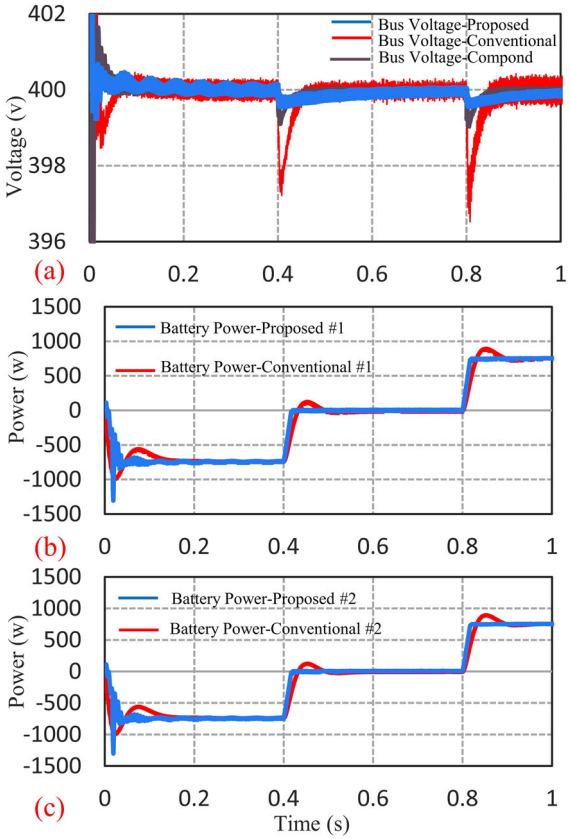

FIGURE 7 Simulation results in the first second: (a) DC bus voltage, (b) battery power #1, (c) battery power #2

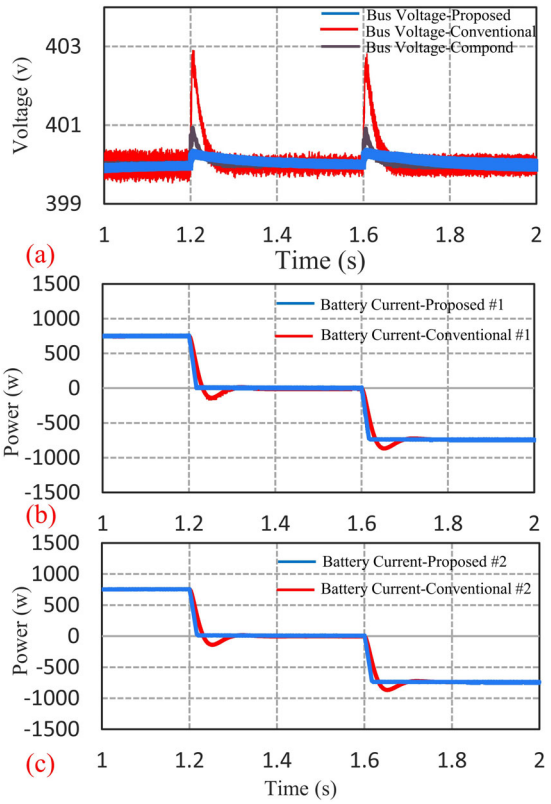

FIGURE 8 Simulation results in the final second: (a) DC bus voltage, (b) battery power #1, (c) battery power #2

simulation results. This table shows the amount of voltage deviation from the reference value. The maximum voltage deviation in the proposed scheme is 0.41484 V, which is much better than other schemes.

7.2 | Performance of virtual supercapacitor based on SOC unit with unbalanced SOC

To evaluate the performance of virtual supercapacitor based on SOC control under simulated SOC imbalance conditions. The load is located in three levels: 12,000 W, 13,500 W, and 15,000 W. The initial values of SOC_1 and SOC_2 are 90% and 80%, respectively. As shown in Figure 9, ESSs are initially in charge mode. SOC_1 increases from 90% to 90.04% in 15 s and SOC_2 from 80% to 80.08%. When the virtual supercapacitor units are in the floating mode. SOC_1 and SOC_2 remain at the same level as before.

According to Figure 10, when manufacturers are unable to meet load demand, virtual supercapacitor units must be discharged. So SOC_1 decreases from 90.04% to. 89.96 and SOC_2 decreases from 80.08% to 80.04% in 45 s. In other words, in the DCMG studied, the batteries are put in three modes: charge, discharge, and standby. When there is the extra power in the DCMG, the batteries are put in charge mode and store this extra power. The controller distributes the power in such a way

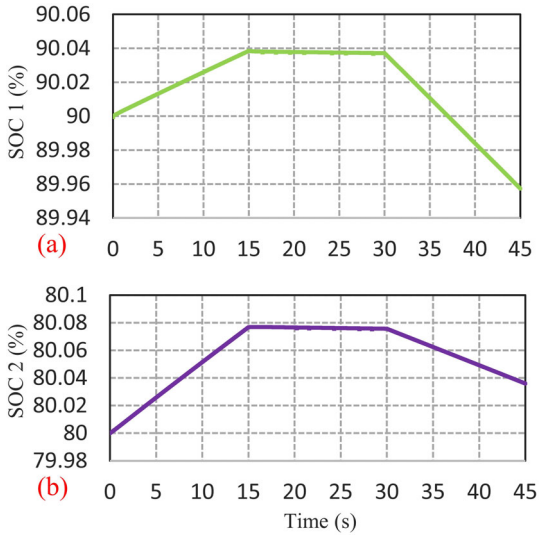

FIGURE 9 (a) SOC 1 (%), (b) SOC 2 (%)

that it provides more power to the battery with a lower charge percentage to charge faster than the other battery, thus trying to balance the SOC of the batteries. The batteries are discharged when DCMG requires additional power. This time, the controller distributes power in such a way that the battery with less charge percentage provides less power to DCMG, thus preventing the battery from being discharged quickly. In the last case,

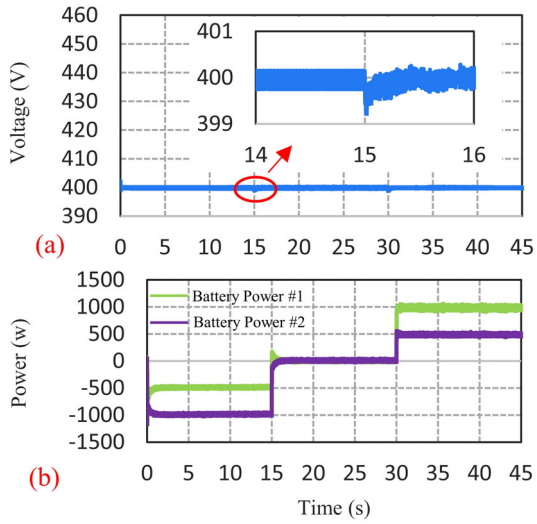

FIGURE 10 (a) DC bus voltage, (b) batteries power

when DCMG does not have extra power or does not need additional power, the batteries are in standby mode and the backup units with DCMG have no power exchange.

8 | CONCLUSIONS

High penetration of RESs has affected the inertia and damping of DCMGs. This problem is solved by the presence of ESSs. To proper operation and high efficiency of the system, the battery should not be charged and discharged continuously. So, DESSs have become a widely accepted concept. In this paper, a virtual supercapacitor based on strategy is proposed by examining inertial emulation methods. Due to the advantages of DHB converter, this converter has been selected for power transmission. Due to the advantages of the DHB converter, this converter has been used as a battery and DCMG interface converter. By analysing and reviewing the simulation results, a positive effect of the proposed strategy can be seen. The proposed scheme, in addition to the correct function in restoring the voltage at load change moments, manages the power exchange at any time by creating a power balance between the ESSs. The deviation of the bus voltage from the reference value is reduced in two modes of voltage drop and voltage increase compared to other common schemes.

CONFLICT OF INTEREST

The authors confirm that this article content has no conflicts of interest.

DATA AVAILABILITY STATEMENT

Data sharing is not applicable to this article as no new data were created or analysed in this study.

ORCID

Hassan Moradi CheshmehBeigi https://orcid.org/0000-0002-4802-6117

REFERENCES

1. Dreidy, M., Mokhlis, H., Mekhilef, S.: Inertia response and frequency control techniques for renewable energy sources: a review. Renew. Sustain. Energy Rev. 69, 144–155 (2017)
2. Dhingra, K., Singh, M.: Frequency support in a micro-grid using virtual synchronous generator based charging station. IET Renew. Power Gener. 12(9), 1034–1044 (2018)
3. Peyghami, S., Palensky, P., Blaabjerg, F.: An overview on the reliability of modern power electronic based power systems. IEEE Open J. Power Electro. 1, 34–50 (2020)
4. Zhu, X., Xie, Z., Jing, S., et al.: Distributed virtual inertia control and stability analysis of dc microgrid. IET Gener. Transm. Distrib. 12(14), 3477–3486 (2018)
5. Dragičević, T., Lu, X., Vasquez, J.C., et al.: DC microgrids – part I: a review of control strategies and stabilization techniques. IEEE Trans. Power Electron. 31(7), 4876–7891 (2016)
6. Al-Ismail, F.S.: 'DC microgrid planning, operation, and control: a comprehensive review. IEEE Access. 9, 36154–36172 (2021)
7. Yi, Z., Zhao, X., Shi, D., et al.: Accurate power sharing and synthetic inertia control for dc building microgrids with guaranteed performance'. IEEE Access. 7, 63698–63708 (2019)
8. Ertugrul, N., Abbott, D.: DC is the future [point of view]. Proc. IEEE. 108(5), 615–624 (2020)
9. Hosseinipour, A., Hojabri, H.: Virtual inertia control of PV systems for dynamic performance and damping enhancement of DC microgrids with constant power loads. IET Ren. Power Gener. 12(4), 430–438 (2018)
10. Fang, J., Li, H., Tang, Y., et al.: On the inertia of future more-electronics power systems. IEEE Trans. Emerg. Sel. 7(4), 2130–2146 (2018)
11. Yang, Y., Li, C., Xu, J., et al.: Virtual inertia control strategy for improving damping performance of DC microgrid with negative feedback effect. IEEE Trans. Emerg. Sel. 9(2), 1241–1257 (2020)
12. Lin, G., Ma, J., Li, Y., et al.: A virtual inertia and damping control to suppress voltage oscillation in islanded DC microgrid. IEEE Trans. Energy Convers. 36(3), 1711–1721 (2020)
13. Zhu, X., Cai, J., Yan, Q., et al.: Virtual inertia control of wind-battery-based islanded DC. In: Int. conf. renewable power Generation (RPG 2015), pp. 1–6. IET Digital Lib., Beijing, China, 17–18 Oct 2015
14. Wu, W., Chen, Y., Luo, A., Zhou, L., et al.: A virtual inertia control strategy for DC microgrids analogized with virtual synchronous machines. IEEE Trans. Power Electron. 64(7), 6005–6016 (2016)
15. Samanta, S., Mishra, J.P., Roy, B.K., et al.: Virtual DC machine: an inertia emulation and control technique for a bidirectional DC–DC converter in a DC microgrid. IET Electron. Power Appl. 12(6), 874–884 (2018)
16. Pishbahar, H., Moradi CheshmehBeigi, H., Piri Yengijeh, N., et al.: Inertia emulation with incorporating the concept of virtual compounded DC machine and bidirectional DC–DC converter for DC microgrid in islanded mode. IET Renew. Power Gener. 15, 1812–1825 (2021)
17. Zhi, N., Ding, K., Du, L., et al.: An SOC-based virtual DC machine control for distributed storage systems in DC microgrids. IEEE Trans. Energy Convers. 35(3), 1411–1420 (2020)
18. Samanta, S., Mishra, J.P., et al.: Implementation of a virtual inertia control for inertia enhancement of a DC microgrid under both grid connected and isolated operation. Comput. Electr. Eng. 76, 283–298 (2019)
19. Zhu, X., Meng, F., Xie, Z., et al.: An inertia and damping control method of DC–DC converter in DC microgrids. IEEE Trans. Energy Convers. 35(2), 799–807 (2019)
20. Jami, M., Shafiee, Q., Gholami, M., et al.: Control of a super-capacitor energy storage system to mimic inertia and transient response improvement of a direct current micro-grid. J. Energy Storage. 32, 10178 (2020)
21. Molina, M.G.: Energy storage and power electronics technologies: a strong combination to empower the transformation to the smart grid. Proc. IEEE. 105(11), 2191–2219 (2017)
22. Koohi-Fayegh, S., Rosen, M.A.: A review of energy storage types, applications and recent developments. J. Energy Storage. 27, 101047 (2020)

23. Lu, X., Guerrero, JM., Sun, K., et al.: Hierarchical control of parallel AC-DC converter interfaces for hybrid microgrids. IEEE Trans. Smart Grid. 5(2), 683–92 (2013)
24. Chowdhury, S.M., Badawy, M.O., Sozer, Y., et al.: A novel battery management system using the duality of the adaptive droop control theory. IEEE Trans. Ind. Appl. 55(5), 5078–5088 (2019)
25. Xing, L., Mishra, Y., Tian, Y.C., et al.: Distributed state-of-charge balance control with event-triggered signal transmissions for multiple energy storage systems in smart grid. IEEE Trans. Syst. 49(8), 1601–1611 (2019)
26. Wang, W., Zhou, M., Jiang, H, et al.: Improved droop control based on state-of-charge in DC microgrid. In: 2020 IEEE 29th international symposium on industrial electronics (ISIE), pp. 1509–1513. Delft, Netherlands, 17–19 Jun 2020. https://doi.org/10.1109/ISIE45063.2020.9152515
27. Oliveira, T.R., Silva, W.W.A.G. Donoso-Garcia, P.F., et al.: Distributed secondary level control for energy storage management in DC microgrids. IEEE Trans. Smart Grid. 8(6), 2597–2607 (2016)
28. Lu, X., Sun, K., Guerrero, J.M., Vasquez, J.C., Huang, L.: State-of-charge balance using adaptive droop control for distributed energy storage systems in DC microgrid applications. IEEE Trans. Ind. Electron. 61(6), 2804–2815 (2013)
29. Lu, X., Sun, K., Guerrero, J.M., et al.: Double-quadrant state-of-charge-based droop control method for distributed energy storage systems in autonomous DC microgrids. IEEE Trans. Smart Grid. 6(1), 147–157 (2014)
30. Mehdipour, A., Farhangi, S.: Comparison of three isolated bidirectional DC/DC converter topologies for a backup photovoltaic application. In: 2011 2nd Int. Conf. electric power and energy conversion systems (EPECS), pp. 1–5. Sharjah, UAE, 15–17 Nov 2011. https://doi.org/10.1109/EPECS.2011.6126822
31. Pan, X., Li, H., Liu, Y., Zhao T, Ju C, Rathore AK, et al.: An overview and comprehensive comparative evaluation of current-fed-isolated-bidirectional DC/DC converter. IEEE Trans. Power Electron. 35(3), 2737–2763 (2019)
32. Inoue, S., Ishigaki, M., Takahashi, A., Sugiyama, T.: Design of an isolated bidirectional DC–DC converter with built-in filters for high power density. IEEE Trans. Power Electron. 36(1), 739–750 (2020)
33. Dominguez, A., Barragan, L.A., Otín, A., Artigas, J.I., Urriza, I., Navarro, D., et al.: Small-signal model of dual half-bridge series resonant inverter sharing resonant capacitor for domestic induction heating. In: IECON 2014 – 40th annual conference of the IEEE Industrial Electronics Society, pp. 3277–3282. Dallas, TX, USA, 29 Oct–1 Nov 2014. https://doi.org/10.1109/IECON.2014.7048981
34. Li, H., Liu, D., Peng, F.Z., et al.: Small signal analysis of a dual half bridge isolated ZVS bi-directional DC-DC converter for electrical vehicle applications. In: 2005 IEEE 36th power electronics specialists conference, pp. 2777–2782. Dresden, Germany, 16 Jun 2005. https://doi.org/10.1109/PESC.2005.1582026

How to cite this article: Piri Yengijeh, N., Moradi CheshmehBeigi, H., Hajizadeh, A.: Inertia emulation with the concept of virtual supercapacitor based on SOC for distributed storage systems in islanded DC microgrid. IET Renew. Power Gener. 16, 2805–2815 (2022). https://doi.org/10.1049/rpg2.12537